

**Q1 Au nanoparticle-functionalised WO<sub>3</sub> nanoneedles and their application in high sensitivity gas sensor devices**

Stella Vallejos, Toni Stoycheva, Polona Umek, Cristina Navio, Rony Snyders, Carla Bittencourt, Eduard Llobet, **Christopher Blackman\*** and Xavier Correig

**Q3** ~~We report a novel vapour phase synthesis for functionalised nanomaterials, applied to producing a high sensitivity gas sensing layer.~~

Please check this proof carefully. **Our staff will not read it in detail after you have returned it.** Translation errors between word-processor files and typesetting systems can occur so the whole proof needs to be read. Please pay particular attention to: tabulated material; equations; numerical data; figures and graphics; and references. If you have not already indicated the corresponding author(s) please mark their name(s) with an asterisk. Please e-mail a list of corrections or the PDF with electronic notes attached -- do not change the text within the PDF file or send a revised manuscript.

**Please bear in mind that minor layout improvements, e.g. in line breaking, table widths and graphic placement, are routinely applied to the final version.**

Please note that, in the typefaces we use, an italic vee looks like this:  $\nu$ , and a Greek nu looks like this:  $\nu$ .

We will publish articles on the web as soon as possible after receiving your corrections; **no late corrections will be made.**

Please return your **final** corrections, where possible within **48 hours** of receipt, by e-mail to: chemcomm@rsc.org

Reprints—Electronic (PDF) reprints will be provided free of charge to the corresponding author. Enquiries about purchasing paper reprints should be addressed via: <http://www.rsc.org/publishing/journals/guidelines/paperreprints/>. Costs for reprints are below:

Reprint costs		
No of pages	Cost (per 50 copies)	
	First	Each additional
2-4	£225	£125
5-8	£350	£240
9-20	£675	£550
21-40	£1250	£975
>40	£1850	£1550
<i>Cost for including cover of journal issue:</i> £55 per 50 copies		

Queries are marked on your proof like this **Q1**, **Q2**, etc. and for your convenience line numbers are indicated like this 5, 10, 15, ...

<b>Query reference</b>	<b>Query</b>	<b>Remarks</b>
Q1	For your information: You can cite this paper before the page numbers are assigned with: (authors), Chem. Commun., (year), DOI: 10.1039/c0cc02398a.	
Q2	Telephone and fax numbers for the corresponding authors were not filled in, would you like to include them?	
Q3	If the contents entry does not fit between the two horizontal lines, then please trim the text and/or the title.	
Q4	A citation for the footnote describing the experimental details has been added, please check its location is suitable.	

# Au nanoparticle-functionalised WO<sub>3</sub> nanoneedles and their application in high sensitivity gas sensor devices†‡

Stella Vallejos,<sup>a</sup> Toni Stoycheva,<sup>a</sup> Polona Umek,<sup>c</sup> Cristina Navio,<sup>d</sup> Rony Snyders,<sup>d</sup> Carla Bittencourt,<sup>d</sup> Eduard Llobet,<sup>a</sup> Christopher Blackman<sup>\*b</sup> and Xavier Correig<sup>a</sup>

Received 6th July 2010, Accepted 10th November 2010

DOI: 10.1039/c0cc02398a

A new method of synthesising nanoparticle-functionalised nanostructured materials via Aerosol Assisted Chemical Vapour Deposition (AACVD) has been developed. Co-deposition of Au nanoparticles with WO<sub>3</sub> nanoneedles has been used to deposit a sensing layer directly onto gas sensor substrates providing devices with a six-fold increase in response to low concentrations of a test analyte (ethanol).

Advances in technology provide new opportunities to exploit the properties of materials at the nanoscale, for instance greatly enhanced reactivities and selectivities have been reported for nanoparticle (NP) catalysts compared to their bulk counterparts,<sup>1</sup> and in NP semiconducting metal oxide (MOX) gas sensors dramatic increases in sensitivity are observed.<sup>2–5</sup> Functionalisation of NP can strongly influence electronic, optical and magnetic properties of the material and the promise of nanotechnology may only ultimately be realised by tailoring the NP properties through introduction of intentional impurities or dopants.<sup>6</sup> This is a very difficult task for nanostructured MOX (nanoneedles, nanoribbons, nanowires, etc.),<sup>7–9</sup> because physical methods of functionalising NP, such as sputtering or evaporation, frequently lead to non-homogeneous coverage and therefore the application of chemical methods in which the NP is synthesised and functionalised in a single step is potentially advantageous. Synthesising NP in the gas phase has potential advantages over liquid phase synthesis including greater purity, continuous mode operation and higher throughput but also presents a number of challenges, including the controlled deposition of nanoparticles onto surfaces and the chemical modification of individual nanoparticles, either to passivate or functionalise their surface.<sup>10</sup> The use of aerosols for NP synthesis is well known and particle size, crystallinity, degree of agglomeration, porosity, chemical homogeneity and stoichiometry can all be controlled with relative ease by adjusting the process parameters.<sup>11</sup> Aerosol

assisted chemical vapour deposition (AACVD) is a variant of traditional CVD in which a precursor solution is transported to the substrate in an aerosol. The nucleation and growth kinetics of nanostructured materials and thin films are influenced by the deposition temperature and concentration of reactive species, which in turn influence the microstructure and thus the properties of the coatings. Nanostructured materials can be obtained by controlling the degree of homogenous and heterogeneous gas-phase reactions,<sup>12</sup> hence by manipulating reaction conditions deposition of nanostructured MOX can be achieved<sup>13–15</sup> and recently the application of AACVD for deposition of metal NP has also been demonstrated.<sup>16,17</sup> Combining these two syntheses together in a single AACVD process could overcome the challenges associated with gas phase NP synthesis by combining the ability to controllably deposit MOX NP onto a surface and the ability to chemically modify these MOX NP by co-deposition with metal NP. This technique, which is expected to be applicable to the synthesis of catalytic NP in general, is of particular relevance for application in MOX gas sensors because these normally respond to a wide range of analytes and functionalisation of these materials with gold or other noble metal particles is required to improve selectivity.<sup>5,9,18</sup> Herein we report the use of AACVD to deposit a NP-functionalised (gold) nanostructured material (WO<sub>3</sub>) and the gas sensing properties of this nanomaterial.

A piezoelectric ultrasonic atomiser was used to generate an aerosol from a precursor mixture (10 mg HAuCl<sub>4</sub>·3H<sub>2</sub>O (Sigma-Aldrich, 99.9%) in 5 cm<sup>3</sup> methanol (Sigma-Aldrich, ≥ 99.6%) and 150 mg W(OPh)<sub>6</sub> (synthesised according to the literature<sup>19</sup>) in 15 cm<sup>3</sup> acetone (Sigma-Aldrich, min. 99.8%)) which was transported to the heated substrate by a nitrogen (Carburos Metálicos, N<sub>2</sub> Premier) gas flow (0.5 l min<sup>-1</sup>). Under these conditions the time taken to transport the entire volume of the solution, *i.e.* the deposition time, was typically 45 min. The substrates were 10 mm × 10 mm × 0.64 mm Al<sub>2</sub>O<sub>3</sub> tiles with inter-digitated Pt electrodes (gap: 300 μm, thickness: 9 μm) on the surface and a Pt heater on the reverse.<sup>20</sup>

To deposit gold NP supported on high surface area nanostructured WO<sub>3</sub> immobilised (*i.e.* adhered) on a substrate, either glass, alumina or silicon, requires precise control of the precursor supersaturation to prevent formation of non-adherent powders or polycrystalline thin films. In this context the choice of precursors is crucial; the gold precursor should decompose at a lower temperature than the MOX precursor to ensure it undergoes homogenous nucleation in the gas phase to form NP, whereas the MOX precursor must undergo some

<sup>a</sup> Departament d'Enginyeria Electrònica, Universitat Rovira i Virgili, Països Catalans 26, 43007 Tarragona, Spain

<sup>b</sup> Department of Chemistry, University College London, 20 Gordon Street, London, WC1H 0AJ, UK. E-mail: c.blackman@ucl.ac.uk Fax: XXXX; Tel: XXXX

<sup>c</sup> Solid State Physics Department, Jožef Stefan Institute, Jamova cesta 39, 1000 Ljubljana, Slovenia

<sup>d</sup> Laboratory of Plasma-Surface Interaction Chemistry (PSI Chem), University of Mons, Av. Nicolas Copernic 1, 7000 Mons, Belgium

† This article is part of the 'Emerging Investigators' themed issue for ChemComm.

‡ Electronic supplementary information (ESI) available: XRD pattern and W 4f, W 5p<sub>3/2</sub> and Au 4f XPS spectra of Au NP/WO<sub>3</sub> nanoneedles are available. See DOI: 10.1039/c0cc02398a

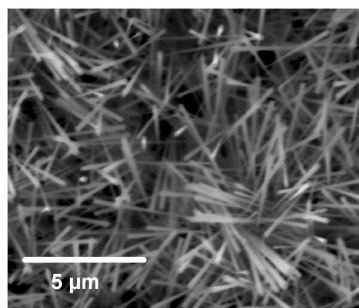


**Fig. 1** SEM image of NP Au/WO<sub>3</sub> NN deposited via AACVD on alumina gas sensor substrate at 350 °C.

degree of heterogeneous reaction on the substrate surface. The substrate temperature required for deposition of the Au NP/WO<sub>3</sub> nanoneedles (NN) was 350 °C; a deposition temperature in excess of 550 °C is required to deposit WO<sub>3</sub> nanoneedles from W(OPh)<sub>6</sub> alone on identical substrates,<sup>21</sup> which indicates the Au NP, or gold precursor, play an active role in the formation of the WO<sub>3</sub> NN. The surface morphology of the as-grown samples (Fig. 1) reveals a high density of non-aligned NN and XRD (supplementary information†) showed the presence of monoclinic WO<sub>3</sub> (*P*<sub>2</sub><sub>1</sub>/*n* space group, *a* = 7.4112(44) Å, *b* = 7.7234(53) Å, *c* = 7.7909(26) Å and *beta* = 91.164°(43) Å; ICDD card no. 72-0677 *a* = 7.30600 Å, *b* = 7.54000 Å, *c* = 7.69200 Å and *beta* = 90.88°) with preferred orientation in the [001] direction. A diffraction peak at 38.184° 2θ is assigned to the (111) plane of gold with the remaining peaks assigned to Al<sub>2</sub>O<sub>3</sub> (corundum) and MgAl<sub>2</sub>O<sub>4</sub> (spinel) from the alumina gas sensor substrates. TEM (Fig. 2) of particles removed from the substrate by sonication in methanol showed the presence of highly monodisperse gold nanoparticles (approximate diameter 11.13 ± 0.19 nm for a total population of 120 particles) randomly dispersed along the surface of the WO<sub>3</sub> NN. HRTEM analysis of Au/WO<sub>3</sub> samples (Fig. 3a) showed the WO<sub>3</sub> crystallites were highly ordered with a planar spacing observed of 0.35–0.37 nm, consistent with an internal order of the WO<sub>3</sub> nanoneedles in the [001] (0.5d = 0.3650 nm) or [020] (0.5d = 0.3770 nm) directions. Crystalline ordering was also observed within the Au particles (Fig. 3b) with the lattice spacing of 0.19 nm corresponding to the (200) plane. Examination of the W 4f and W 5p<sub>3/2</sub> core level XPS spectrum (supplementary information†) of Au/WO<sub>3</sub> samples compared to a WO<sub>3</sub> thin film standard showed no difference in the peak positions,

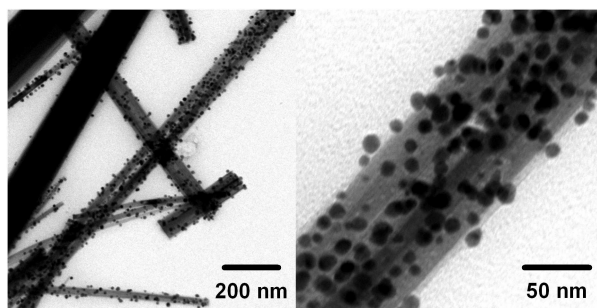


**Fig. 2** TEM images of WO<sub>3</sub> NN with dispersed gold NP on the surface; (a) overview and (b) detailed view.

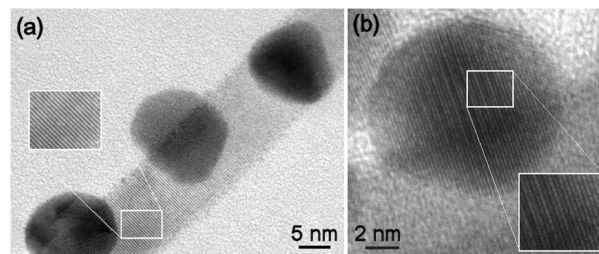


**Fig. 3** HRTEM images of (a) WO<sub>3</sub> NN with Au NP on surface and (b) close-up of Au NP.

indicating only a weak interaction between the WO<sub>3</sub> NN and the co-deposited Au NP. The peak broadening observed in the Au/WO<sub>3</sub> sample is associated with the presence of surface defects in the WO<sub>3</sub> NN which become quantitatively important in the XPS spectrum due to the higher surface area of the WO<sub>3</sub> NN compared with the WO<sub>3</sub> thin film standard.<sup>22</sup> Examination of the Au 4f core level (supplementary information†) showed the deposited Au NP were metallic, again indicating only a weak electronic interaction with the WO<sub>3</sub> NN.

The gas sensing characterization was carried out by monitoring the resistance change of the Au/WO<sub>3</sub> samples during exposure to trace concentrations of ethanol in a continuous flow test chamber.<sup>23</sup> Several sensor operating temperatures in the range 150–350 °C were tested. A maximum sensor response to 1.5 ppm of ethanol was achieved at an operating temperature of 250 °C, a typical resistance response for these conditions is displayed in Fig. 4. The Au/WO<sub>3</sub> samples gave a high sensor response (*S<sub>R</sub>* = 12) to low concentrations (1.5 ppm) of ethanol. In a previous study AACVD deposited undoped WO<sub>3</sub> NN had relatively much lower sensitivities (*S<sub>R</sub>* = 2) to ethanol concentrations up to 20 ppm and functionalisation of the WO<sub>3</sub> NN by sputtering with Au provided no increase in sensitivity.<sup>21</sup> AACVD co-deposition of Au NP with WO<sub>3</sub> NN provides a six-fold increase in the sensitivity of the WO<sub>3</sub> towards low concentrations of ethanol compared to either AACVD deposited WO<sub>3</sub> NN or WO<sub>3</sub> NN decorated with sputtered Au. The Au NP enhance sensitivity over non-functionalised WO<sub>3</sub> NN by promoting reactions at the surface of the MOX and by altering the Fermi energy of the system through the metal/semiconductor interface. In

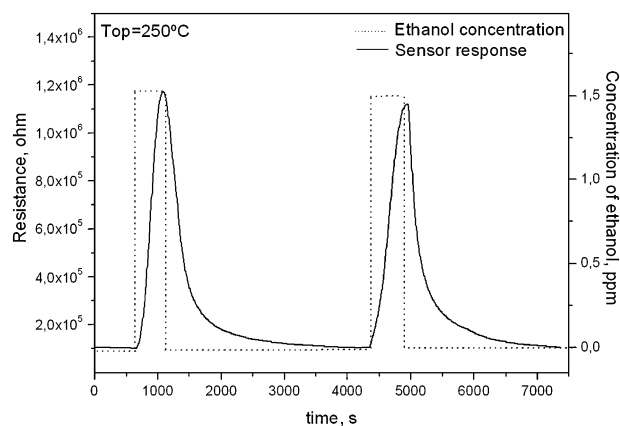


**Fig. 4** Typical gas sensor response to 1.5 ppm of ethanol at operating temperature of 250 °C.

sputtered samples agglomeration of Au NP particles is observed, the enhanced sensitivity of the AACVD co-deposited material is therefore ascribed to the smaller size and higher dispersity of the Au NP, both factors which are known to promote sensitivity.<sup>1,9</sup> Of particular interest is the Au/WO<sub>3</sub> samples in this study show an increase in electrical resistance when exposed to ethanol, whereas WO<sub>3</sub> gas sensors normally show a reduction in resistance. A similar behaviour has recently been reported for TeO<sub>2</sub> nanowire<sup>24</sup> and WO<sub>3</sub> nanorod<sup>25</sup> based gas sensors upon exposure to ethanol. The effect is attributed to ethanol behaving as an oxidative gas under certain conditions of concentration and temperature,<sup>24,26</sup> which causes a change in the Fermi energy of the MOX hence forming an inversion layer at the surface. This change from n- to p-type conduction becomes dominant in MOX NN due to the comparable dimensions between the mean free path of the carriers and the diameter of the NN.<sup>27,28</sup> An important factor in the performance of a gas sensor is long term stability under operating conditions. After the gas sensing experiments, running through a month at temperatures up to 350 °C and in several environments (NO<sub>2</sub>, CO, NH<sub>3</sub>), the Au/WO<sub>3</sub> samples were examined again using ESEM and TEM. In comparison to the initial samples the morphology of the WO<sub>3</sub> NN was unchanged and the dispersion and size of the Au NP were identical, indicating the potential of these materials for application in gas sensor devices.

In conclusion, a methodology for the co-deposition of WO<sub>3</sub> NN and Au NP *via* AACVD has been developed and used to deposit Au/WO<sub>3</sub> samples directly onto gas sensor substrates. These gas sensors have high sensitivities to low concentrations (1.5 ppm) of ethanol and the measured change in electrical resistance is enhanced compared to traditional WO<sub>3</sub>-based gas sensors. AACVD has previously been used to deposit not only nanostructured WO<sub>3</sub><sup>22</sup> but also nanostructured In<sub>2</sub>O<sub>3</sub>,<sup>14</sup> ZnO<sup>29</sup> and MoS<sub>2</sub>,<sup>30</sup> and the ability to use either NP precursors or preformed NP (deposition of Al, Cu and Ag particles<sup>31</sup> as well as Au particles<sup>16</sup> has already been reported) indicates AACVD could provide a simple and flexible way to directly deposit nanostructured materials functionalised with metal NP onto defined surfaces for use in catalysis and gas sensing.

This work is partially supported by the Belgian Program on Interuniversity Attraction Pole (PAI 6/08) and ARC-UMONS and by the Spanish project TEC2009-07107 funded by MICINN. The support of the COST Action MP0901 “NanoTP” is gratefully acknowledged. CB and SV are grateful for the support of the Leverhulme Trust *via* Research Project Grant F/07 134/DB.

## Notes and references

§ The morphology of the Au NP/WO<sub>3</sub> NN was examined using Environmental Scanning Electron Microscopy (ESEM-FEI Quanta 600) and Transmission Electron Microscopy (TEM—JEOL 1011), the structure using X-ray Diffraction (XRD—Bruker-AXS D8-Discover) and High Resolution TEM (HRTEM—Jeol 2100) and the chemical composition using X-ray Photoelectron Spectroscopy (XPS—Physical Electronics-VERSAPROBE PHI 5000, using monochromatic Al K $\alpha$

radiation with 0.6 eV energy resolution; dual beam charge neutralization from an electron gun (~1 eV) and argon ion gun ( $\leq 10$  eV) was used for charge compensation). For the gas sensor measurements the sensor was exposed to 1.5 ppm ethanol for 10 min and subsequently the chamber (gas flow: 200 sccm, chamber volume: 280 cm<sup>3</sup>) purged with air until the initial baseline resistance was recovered. To obtain the desired analyte concentration a calibrated ethanol gas standard in synthetic air (Carbueros Metálicos, 19.9 ppm  $\pm$  1 ppm) was mixed with pure dry air (Carbueros Metálicos, 99.99%). The sensor response was defined as  $SR = R_{\text{gas}}/R_{\text{air}}$ , where  $R_{\text{air}}$  is the sensor resistance in air at stationary state and  $R_{\text{gas}}$  represents the sensor resistance after 10 min of ethanol exposure.

- 1 B. R. Cuenya, *Thin Solid Films*, 2010, **518**, 3127–3150.
- 2 N. Yamazoe, *Sens. Actuators, B*, 1991, **5**, 7–19.
- 3 N. Barsan and U. Weimar, *J. Electroceram.*, 2001, **7**, 143–167.
- 4 A. Rothschild and Y. Komem, *J. Appl. Phys.*, 2004, **95**, 6374–6380.
- 5 M. E. Franke, T. J. Koplin and U. Simon, *Small*, 2006, **2**, 36–50.
- 6 D. J. Norris, A. L. Efros and S. C. Erwin, *Science*, 2008, **319**, 1776–1779.
- 7 E. Comini, C. Baratto, G. Faglia, M. Ferroni, A. Vomiero and G. Sberveglieri, *Prog. Mater. Sci.*, 2009, **54**, 1–67.
- 8 X. Fang, L. Hu, C. Ye and L. Zhang, *Pure Appl. Chem.*, 2010, **82**, 2185–2198.
- 9 A. Kolmakov, X. H. Chen and M. Moskovits, *J. Nanosci. Nanotechnol.*, 2008, **8**, 111–121.
- 10 S. L. Girshick, *J. Nanopart. Res.*, 2008, **10**, 935–945.
- 11 M. T. Swihart, *Curr. Opin. Colloid Interface Sci.*, 2003, **8**, 127–133.
- 12 K. L. Choy, *Prog. Mater. Sci.*, 2003, **48**, 57–170.
- 13 S. Ashraf, C. S. Blackman, R. G. Palgrave, S. C. Naisbitt and I. P. Parkin, *J. Mater. Chem.*, 2007, **17**, 3708–3713.
- 14 S. Basharat, C. J. Carmalt, S. A. Barnett, D. A. Tocher and H. O. Davies, *Inorg. Chem.*, 2007, **46**, 9473–9480.
- 15 C. S. Blackman, X. Correig, V. Khatko, A. Mozalev, I. P. Parkin, R. Alcobilla and T. Trifonov, *Mater. Lett.*, 2008, **62**, 4582–4584.
- 16 R. G. Palgrave and I. P. Parkin, *J. Am. Chem. Soc.*, 2006, **128**, 1587–1597.
- 17 R. G. Palgrave and I. P. Parkin, *Chem. Mater.*, 2007, **19**, 4639–4647.
- 18 M. Stankova, X. Vilanova, J. Calderer, E. Llobet, J. Brezmes, I. Gràcia, C. Cané and X. Correig, *Sens. Actuators, B*, 2006, **113**, 241–248.
- 19 W. B. Cross, I. P. Parkin, S. A. O'Neill, P. A. Williams, M. F. Mahon and K. C. Molloy, *Chem. Mater.*, 2003, **15**, 2786–2796.
- 20 P. Ivanov, J. Hubalek, K. Malysz, J. Prásek, X. Vilanova, E. Llobet and X. Correig, *Sens. Actuators, B*, 2004, **100**, 221–227.
- 21 T. Stoycheva, S. Vallejos, J. Calderer, I. Parkin, C. Blackman and X. Correig, *Procedia Engineering*, 2010, **5**, 131–134.
- 22 J. Huang and Q. Wan, *Sensors*, 2009, **9**, 9903–9924.
- 23 V. Khatko, S. Vallejos, J. Calderer, I. Gracia, C. Cané, E. Llobet and X. Correig, *Sens. Actuators, B*, 2009, **140**, 356–362.
- 24 T. Siciliano, A. Tepore, G. Micocci, A. Genga, M. Siciliano and E. Filippo, *Sens. Actuators, B*, 2009, **138**, 207–213.
- 25 Y. S. Kim, S. C. Ha, K. Kim, H. Yang, S. Y. Choi, Y. T. Kim, J. T. Park, C. H. Lee, J. Choi, J. Paek and K. Lee, *Appl. Phys. Lett.*, 2005, **86**, 3.
- 26 T. Wolkenstein, *Electronic Processes on Semiconductor Surfaces during Chemisorption*, Consultants Bureau, New York, 1991.
- 27 A. Gurlo, N. Barsan, A. Oprea, M. Sahn, T. Sahn and U. Weimar, *Appl. Phys. Lett.*, 2004, **85**, 2280–2282.
- 28 A. Gurlo, M. Sahn, A. Oprea, N. Barsan and U. Weimar, *Sens. Actuators, B*, 2004, **102**, 291–298.
- 29 M. R. Waugh, G. Hyett and I. P. Parkin, *Chem. Vap. Deposition*, 2008, **14**, 366–372.
- 30 A. Adeogun, M. Afzaal and P. O'Brien, *Chem. Vap. Deposition*, 2006, **12**, 597–599.
- 31 G. Walters and I. P. Parkin, *Appl. Surf. Sci.*, 2009, **255**, 6555–6560.